Ion-induced nucleation in polar one-component fluids

Kitamura, H; Onuki, A

THE JOURNAL OF CHEMICAL PHYSICS **123**, 124513 (2005)

Ion-induced nucleation in polar one-component fluids

Hikaru Kitamura[a] and Akira Onuki
Department of Physics, Kyoto University, Kyoto 606-8502, Japan

(Received 13 December 2004; accepted 27 July 2005; published online 27 September 2005)

We present a Ginzburg-Landau theory of ion-induced nucleation in a gas phase of polar one-component fluids, where a liquid droplet grows with an ion at its center. By calculating the density profile around an ion, we show that the solvation free energy is larger in gas than in liquid at the same temperature on the coexistence curve. This difference much reduces the nucleation barrier in a metastable gas. © *2005 American Institute of Physics*. [DOI: 10.1063/1.2039078]

I. INTRODUCTION

Ion-induced nucleation in water vapor plays a decisive role in many atmospheric phenomena. It is well known that the nucleation rate is much enhanced in polar fluids in the presence of ions.[1,2] However, precise experiments on this effect have been difficult despite the long history of this problem since Wilson's cloud chamber experiment.[1,3,4] Theoretically, we need to understand the statistical behavior of polar molecules around an ion[5] and the heterogeneous nucleation triggered by such ion-dipole interaction in metastable states. This problem is thus of fundamental importance in physics and chemistry, but it has rarely been studied in literature.

Originally, Thomson[2] calculated the chemical potential of vapor in the vicinity of a charged particle using continuum electrostatics and predicted the formation of a small liquid droplet with the ion at its center. However, its radius is only 3 Å in room-temperature water vapor, so Thomson's picture is an oversimplified one. Recently, ion-induced nucleation has been studied using a density-functional theory,[6,7] a Monte Carlo method,[8] and molecular-dynamics simulations.[9] These numerical studies have shown clustering of polar molecules around an ion and alignment of the dipoles along the electric field. After the statistical average, the first effect gives rise to a density inhomogeneity $n(r)$ or electrostriction around an ion. It is worth noting that Born calculated the solvation free energy due to an ion in continuum electrostatics, accounting for polarization alignment (in the linear response) but neglecting electrostriction.[5,10,11]

The aim of this work is to present a Ginzburg-Landau theory of ion-induced nucleation in polar one-component fluids in a gas phase. It will be based on our recent theory of solvation effects in near-critical polar binary mixtures.[12,13] Our theory will take into account both electrostriction and polarization alignment. As will be discussed, the Born formula becomes a poor approximation in strong electrostriction, particularly when an ion is in gaseous polar fluids. The merits of our approach are its simplicity and its ability to describe mesoscopic effects such as nucleation. In Sec. II a theoretical background of solvation will be presented. In Sec. III the free energy increase to create a critical droplet around an ion will be calculated in a gaseous polar fluid.

II. THEORETICAL BACKGROUND

A. Electrostatics

We place a charged particle (ion) in a polar one-component fluid. We assume that the static dielectric constant $\varepsilon=\varepsilon(n)$ is an increasing function of the fluid density n at each temperature T. In the continuum approximation the electric field $\boldsymbol{E}=-\nabla\Phi$ is induced by the electric charge and the electric potential Φ satisfies

$$\nabla\cdot\varepsilon\,\nabla\,\Phi=-4\pi\rho(\boldsymbol{r}), \tag{2.1}$$

where $\rho(\boldsymbol{r})$ is the charge density. Here the polarization $\boldsymbol{P}$ is assumed to be aligned along $\boldsymbol{E}$ as $\boldsymbol{P}=\chi\boldsymbol{E}$, with $\chi=(4\pi)^{-1}(\varepsilon-1)$ being the polarizability.[11] We take the origin of the reference frame at the center of the ion. It is convenient to assume that the charge density is homogeneous within a sphere $r<R_i$ as

$$\rho=Ze/(4\pi R_i^3/3)\quad(r<R_i) \tag{2.2}$$

and vanishes outside the sphere $r>R_i$. The total charge is given by Ze. In our theory R_i is a phenomenological parameter representing the ion radius.[14] Then $n=n(r)$ and $\Phi=\Phi(r)$ depend only on $r=|\boldsymbol{r}|$. In this case Eq. (2.1) is solved to give

$$-\varepsilon(n)\Phi'(r)=\frac{4\pi}{r^2}\int_0^r dr_1 r_1^2\rho(r_1)=\frac{Ze}{r^2}\theta(r), \tag{2.3}$$

where $\Phi'(r)=d\Phi(r)/dr$, $\theta(r)=1$ for $r>R_i$ and

$$\theta(r)=(r/R_i)^3\quad(r<R_i). \tag{2.4}$$

The electrostatic free energy is simply of the following form:[11]

$$F_e=\int d\boldsymbol{r}\frac{1}{8\pi}\varepsilon\boldsymbol{E}^2=\frac{1}{2}Z^2e^2\int_0^\infty dr\frac{1}{\varepsilon r^2}\theta(r)^2. \tag{2.5}$$

Its functional derivative with respect to n yields the chemical potential contribution arising from the electrostatic interaction,

[a]Electronic mail: kitamura@scphys.kyoto-u.ac.jp

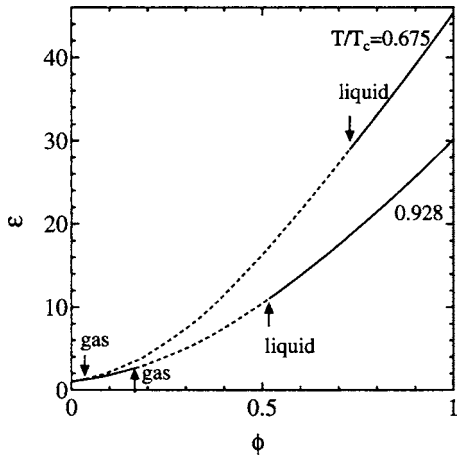

FIG. 1. Static dielectric constant ε as a function of $\phi=v_0 n$ at $T/T_c=0.675$ and 0.928 on the basis of the Harris-Alder formula (2.7) using the data water in Ref. 17. The dotted part corresponds to the two-phase region in the van der Waals model and is given by $0.0358<\phi<0.729$ for $T/T_c=0.675$ and by $0.168<\phi<0.519$ for $T/T_c=0.928$.

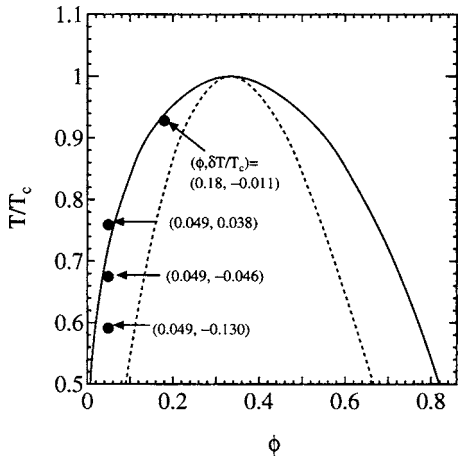

FIG. 2. Phase diagram in the plane of T/T_c and $\phi=v_0 n$ with coexistence curve (solid line) and spinodal curve (dotted line). Use is made of the van der Waals model. At the dots (●) numerical calculations are performed in this work.

$$\mu_e=\frac{\delta}{\delta n}F_e=-\frac{Z^2e^2\varepsilon'}{8\pi\varepsilon^2}\frac{\theta(r)^2}{r^4}, \tag{2.6}$$

where $\varepsilon'=(\partial\varepsilon/\partial n)_T$. This quantity is negative and grows strongly as r approaches R_i, leading to the accumulation of the fluid particles around the ion. Here we are neglecting the nonlinear electric-field effect near the ion[7,15,16] (see the discussion in Sec. IV). The effect arising from the complex molecular structure of solvent molecules is also beyond the scope of this work, which leads to the dependence of the nucleation rate on the sign of the charge of ions.[7]

A number of theories have been presented to describe the overall density and temperature dependence of the dielectric constant $\varepsilon=\varepsilon(n,T)$. Recently, Fernandez *et al.*[17] analyzed a wide range of data on ε for water and steam using the formula proposed by Harris and Alder[18] for polarizable polar fluids,

$$\frac{\varepsilon-1}{\varepsilon+2}=4\pi n\left[\frac{\alpha_m}{3}+\frac{g\mu^2}{k_BT}\frac{\varepsilon}{(2\varepsilon+1)(\varepsilon+2)}\right], \tag{2.7}$$

where α_m represents the molecular polarizability and μ is the dipole moment of a molecule ($\sim$2 D for water). This form is reduced to the Clausius-Mossotti formula in the absence of a permanent dipole and tends to the Kirkwood formula $(\varepsilon-1)(2\varepsilon+1)/\varepsilon=4\pi n g\mu^2/k_BT$ for nonpolarizable molecules with permanent dipole moment.[19] Here g is the so-called Kirkwood correlation factor arising from the correlation between the molecular orientations due to nondipolar interactions (2–3 for liquid water), so g weakly depends on n as revealed in experiments.[20] In Fig. 1 we plot ε as a function of n at $T/T_c=0.675$($T=437$ K) and 0.928 ($T=600$ K) below T_c on the basis of the formula (2.7) using the data on α_m and $g\mu^2$ for water in Ref. 17. In our numerical analysis the quantity $\varepsilon'/\varepsilon^2$ in Eq. (2.6) will be calculated using the formula (2.7).

B. Ginzburg-Landau free energy

For simplicity we use the Helmholtz free-energy density $f=f(n,T)$ in the van der Waals theory,[21]

$$f=k_BTn\ln\left[\frac{\lambda_{\rm th}^3 n}{1-v_0 n}\right]-k_BTn-4\epsilon_{\rm vw}v_0n^2, \tag{2.8}$$

where v_0 and $\epsilon_{\rm vw}$ represent the molecular hard-core volume and the strength of the attractive part of the pair interaction, respectively, and $\lambda_{\rm th}=\hbar(2\pi/mk_BT)^{1/2}$ is the thermal de Broglie length. It follows the well-known expression for the van der Waals pressure,

$$p=n\mu-f=\frac{k_BTn}{1-v_0n}-4\epsilon_{\rm vw}v_0n^2, \tag{2.9}$$

where $\mu=\partial f/\partial n$ is the chemical potential per particle of the form

$$\mu=k_BT\ln\left[\frac{\lambda_{\rm th}^3}{1-v_0n}\right]+\frac{k_BTv_0n}{1-v_0n}-8\epsilon_{\rm vw}v_0n. \tag{2.10}$$

The isothermal compressibility K_T behaves as

$$nk_BK_T=(1-v_0n)^2/[T-T_s(n)], \tag{2.11}$$

where $T_s(n)$ is the spinodal temperature given by

$$T_s(n)=8\epsilon_{\rm vw}v_0n(1-v_0n)^2/k_B. \tag{2.12}$$

The maximization of $T_s(n)$ with respect to n gives the critical temperature and density,

$$T_c=32\epsilon_{\rm vw}/27k_B,\quad n_c=1/3v_0. \tag{2.13}$$

In Fig. 2 we show the phase diagram in the T-ϕ plane for the van der Waals fluid, where $\phi=v_0n$ is the normalized density or the volume fraction of the hard-core region. In this work we will set $v_0=30.96\times10^{-24}$ cm^3 and $\epsilon_{\rm vw}/k_B=545.98$ K, which follow from the critical values $n_c=1.076\times10^{22}$ cm^{-3} and $T_c=647.096$ K for water.[22,23] We introduce the van der Waals radius,

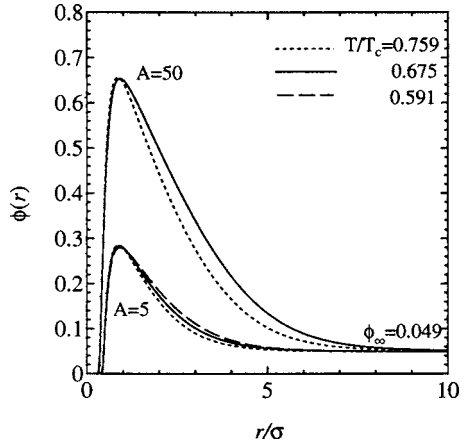

FIG. 3. Normalized density $\phi(r)=v_0 n(r)$ around an ion in the gas phase ($\phi_\infty=v_0 n_\infty=0.049$) close to the coexistence curve ($T_{cx}=0.721$) for $A=5$ and 50. The data are for the three dots with $\phi=0.049$ in Fig. 2. The curves for $T/T_c=0.759$ represent stable profiles, while the others metastable ones. However, for $T/T_c=0.591$ and $A=50$, there is no metastable solution with $\lim_{r\to\infty} n(r)=n_\infty$.

$$\sigma = v_0^{1/3}, \tag{2.14}$$

which is 3.1 Å for water.

We assume that n tends to a homogeneous value n_∞ far from the ion $r\to\infty$ and that the temperature T is homogeneous throughout the system. These assumptions are allowable in calculating the equilibrium solvation profile and the critical droplet in nucleation.[24] The chemical potential and the pressure far from the ion are written as μ_∞ and p_∞, respectively. We consider the grand potential Ω (equal to $-pV$ for homogeneous states) at the temperature T and the chemical potential $\mu=\mu_\infty$. Its increase due to an ion including the gradient and electrostatic contributions is written as

$$\Delta\Omega = \int d\boldsymbol{r}\left[g + \frac{C}{2}|\nabla n|^2 + \frac{\epsilon}{8\pi}\boldsymbol{E}^2 \right], \tag{2.15}$$

where C is a constant and

$$g(n) = f(n) - \mu_\infty n + p_\infty = f(n) - f_\infty - \mu_\infty(n-n_\infty), \tag{2.16}$$

with f_∞ being the Helmholtz free-energy density far from the ion. The $\Delta\Omega$ will be called the solvation free energy. Here g and $\partial g/\partial n$ tend to zero at $n\to n_\infty$, so that we have $g\cong(n-n_\infty)^2/2n_\infty^2 K_T(n_\infty)$ far from the ion. It is worth noting that if the electrostriction is neglected or $n=n_\infty$ in the whole space, $\Delta\Omega$ consists of the electrostatic free energy F_e only, leading to the Born contribution,[11]

$$\Delta\Omega_{\rm Born} = \int d\boldsymbol{r}\frac{\varepsilon_\infty}{8\pi}\left(\frac{Ze}{\varepsilon_\infty r^2}\right)^2 = \frac{Z^2e^2}{2\varepsilon_\infty R_B}, \tag{2.17}$$

where $\varepsilon_\infty=\varepsilon(n_\infty)$. Here $R_B=R_i$ if the space integral is outside the ion ($r>R_i$) (Ref. 25) with the upper bound pushed to infinity. However, this contribution much overestimates F_e when $n(r)$ approaches a liquid density close to the ion and tends to a smaller (gas or supercritical) density far from it. In such cases F_e is of the order $Z^2e^2/2\varepsilon_\ell R_B$, with ε_ℓ being the dielectric constant in liquid,[13] which is much smaller than $\Delta\Omega_{\rm Born}$ in Eq. (2.17) for $\varepsilon_\ell \gg \varepsilon_\infty$.

In Eq. (2.15) F_e arises from the ion-dipole interaction among the ion and the solvent molecules. However, there is also a repulsive interaction among them. To account for it we may include a potential $v_{\rm is}(r)$ to obtain another form of the grand potential increase given by

$$\Delta\Omega' = \Delta\Omega + \int d\boldsymbol{r} v_{\rm is}(r) n(r), \tag{2.18}$$

as in the density-functional theory in Ref. 6. The potential $v_{\rm is}(r)$ should grow strongly close to the ion center. In this paper we use the truncated Lenard-Jones potential $v_{\rm is}$ defined by

$$v_{\rm is}(r) = \epsilon_{\rm vw}[(\sigma_{\rm is}/r)^{12} - (\sigma_{\rm is}/r)^6] \quad (r<\sigma_{\rm is}), \tag{2.19}$$

and $v_{\rm is}(r)=0$ for $r>\sigma_{\rm is}$ with $\sigma_{\rm is}=\sigma/2+R_i$. We will show numerical results starting with either Eq. (2.15) or Eq. (2.18).

In this paper the coefficient C of the gradient term in Eq. (2.15) will be set equal to

$$C = 10\sigma^5 k_B T. \tag{2.20}$$

As will be shown in Appendix A, this choice of C is consistent with a calculation of the surface tension γ for water in Ref. 23. The thermal correlation length $\xi=(Cn^2K_T)^{1/2}$ is then about σ for $T/T_c=0.675$ and about 2.2σ for $T/T_c=0.928$ in liquid on the coexistence curve.

C. Solvation in gas

When an ion solvates the surrounding fluid in stable or metastable one-phase states, we may determine the density profile $n=n(r)$ by requiring the extremum condition $\delta\Delta\Omega/\delta n=0$ or $\delta\Delta\Omega'/\delta n=0$ expressed as

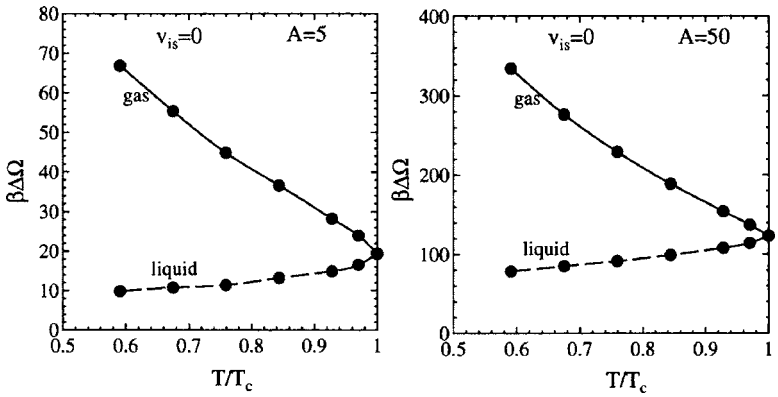

FIG. 4. Normalized solvation free energy $\beta\Delta\Omega$ without $v_{\rm is}$ around an ion for gas and liquid on the coexistence curve for $A=5$ (left) and 50 (right).

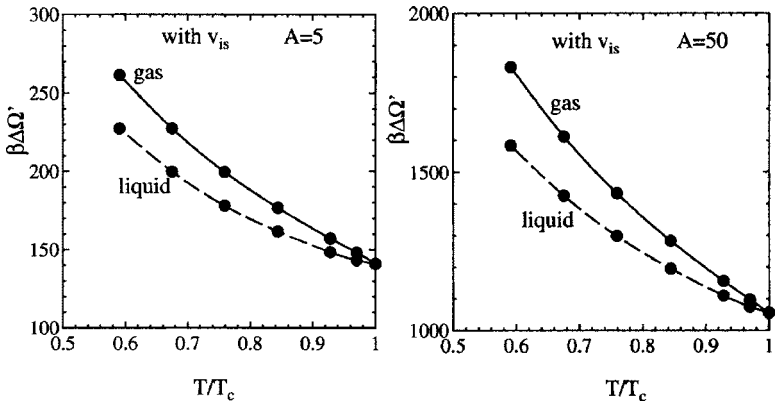

FIG. 5. Normalized solvation free energy $\beta\Delta\Omega'$ with v_{is} around an ion for gas and liquid on the coexistence curve for $A=5$ (left) and 50 (right).

$$\tilde{\mu} - C\nabla^2 n - \mu_\infty = \epsilon_{vw} A\sigma \frac{\varepsilon' \theta^2}{\varepsilon^2 r^4}, \tag{2.21}$$

where $\tilde{\mu}$ is equal to μ in Eq. (2.10) for $\delta\Delta\Omega/\delta n=0$ or to $\mu+v_{is}$ for $\delta\Delta\Omega'/\delta n=0$. The right-hand side is μ_e in Eq. (2.6). We introduce the dimensionless strength of the electric field,

$$A = \frac{Z^2 e^2}{8\pi\sigma\epsilon_{vw}} = \frac{4}{27\pi}\frac{Z^2 e^2}{\sigma k_B T_c}, \tag{2.22}$$

using ϵ_{vw} in Eq. (2.8) or T_c in Eq. (2.13). Here we estimate $A=3.9Z^2$ for water. As shown in our previous work,[13] the gradient term becomes negligible in Eq. (2.21) far from the ion. The long-distance behavior of the deviation $\delta n=n-n_\infty$ far from the critical point is

$$\delta n \cong D_\infty \epsilon_{vw} A\sigma/r^4 \quad (r \gg \sigma), \tag{2.23}$$

with D_∞ being the value of $n^2 K_T \varepsilon'/\varepsilon^2$ far from the ion. The solvation profile is more complicated near the critical point due to the growing correlation length.[13]

In numerically solving Eq. (2.21) the ion radius will be assumed to be given by

$$R_i = 0.3\sigma. \tag{2.24}$$

which is taken to be considerably smaller than σ and then $\sigma_{is}=0.8\sigma$ in Eq. (2.19). In literature[5,14] the ion radius has been estimated for various ions in water. For example, in Table V in Ref. 5, the *bare* ion radii are approximately 0.68 Å for Li^+, 0.95 Å for Na^+, 1.69 Å for Cs^{2+}, and 0.5 Å for Al^{3+}, which are considerably smaller than the corresponding hydration shell radii. The bare radius in Ref. 5 corresponds to R_i in our theory.

In Fig. 3 we show the normalized density profile $\phi(r)=v_0 n(r)$ around an ion in the gas-phase case $\phi_\infty=v_0 n_\infty=0.049$ for $A=5$ and 50 by minimizing $\Delta\Omega'$ in Eq. (2.18), including v_{is}. Note that $n(r)$ tends to zero rapidly at small r. Similar density profiles were calculated in the previous studies.[6,8,9] On the other hand, if we minimize $\Delta\Omega$ in Eq. (2.15) without v_{is}, $n(r)$ tends to a positive constant $n(0)$ at small $r<R_i$, as for the concentration in our previous work.[13] We show that the solvation density profiles change continuously close to the coexistence curve with a change in the temperature difference,

$$\delta T = T - T_{cx}, \tag{2.25}$$

where T_{cx} is the coexistence temperature at a given density. This means that there is no discontinuous change in the solvation profile and the free energy near the coexistence curve.[26]

Let us consider the condition of strong electrostriction in the gas phase, where $n(r)$ assumes a liquid density close to an ion. Note that the chemical potential on the left-hand side of Eq. (2.21) is of the order $k_B T/(1-v_0 n)$ and ε' is of the order $v_0\varepsilon$ in liquid states with $k_B T \sim \epsilon_{vw}$ and $n \sim v_0^{-1}$. Thus strong solvation condition is given by

$$A(\sigma/R_i)^4/\varepsilon_\ell \gg 1, \tag{2.26}$$

where ε_ℓ is the dielectric constant in liquid. The degree of solvation strongly increases with decreasing relative ion size R_i/σ, as is well known in the literature.[5] The shell radius R_{shell} may be defined such that $n(r)$ is on the order of the

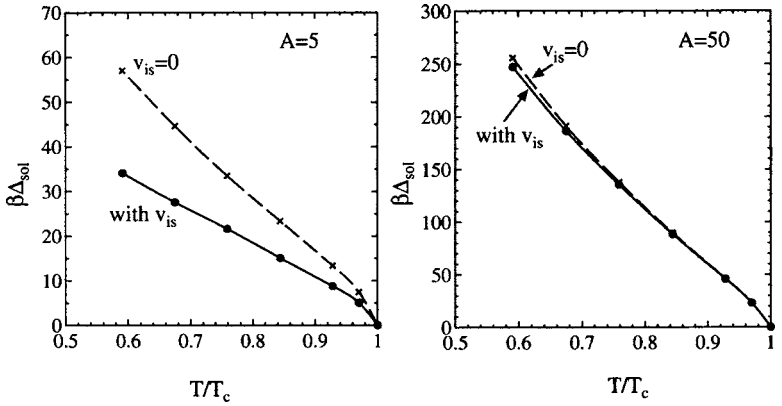

FIG. 6. Normalized solvation free energy difference $\beta\Delta_{sol}$ defined by Eq. (3.5) along the coexistence curve with and without v_{is} for $A=5$ (left) and 50 (right).

liquid density within the shell region $r<R_{\rm shell}$. Then we find $A(\sigma/R_{\rm shell})^4/\varepsilon_\ell \sim 1$ to obtain

$$R_{\rm shell} \sim \sigma(A/\varepsilon_\ell)^{1/4}, \tag{2.27}$$

which can exceed σ for $A/\varepsilon_\ell \gtrsim 1$.

D. Solvation on the coexistence curve

Due to the large density variation around an ion in gas, the effect of electrostriction is more marked in gas than in liquid. As a result, the solvation free energy is larger in gas than in liquid on the coexistence curve. We show $\beta\Delta\Omega$ without $\upsilon_{\rm is}$ in Fig. 4 and $\beta\Delta\Omega'$ with $\upsilon_{\rm is}$ in Fig. 5 for the two phases along the coexistence curve. We notice that $\beta\Delta\Omega'$ even exceeds 1000 on the right panel of Fig. 5. This is because $\varepsilon(n)$ decreases from a liquid value to a gas value in the region $r<\sigma_{\rm is}$ in the presence of $\upsilon_{\rm is}$. As a result, the integration of the electrostatic energy density in the region $R_i<r<\sigma_{\rm is}$ becomes of the order $\Delta\Omega_{\rm Born}$ in Eq. (2.17) ($\sim 10^3 k_BT$ for $A=50$).

In Sec. III we shall see that relevant in nucleation is the difference between the gas value and the liquid value of the solvation free energy,

$$\Delta_{\rm sol} = \begin{cases} (\Delta\Omega)_{n=n_g} - (\Delta\Omega)_{n=n_\ell} & \text{without } \upsilon_{\rm is}, \\ (\Delta\Omega')_{n=n_g} - (\Delta\Omega')_{n=n_\ell} & \text{with } \upsilon_{\rm is}. \end{cases} \tag{2.28}$$

Here the grand-potential increases, $\Delta\Omega$ and $\Delta\Omega'$, are calculated using the inhomogeneous solutions of Eq. (2.21), $n=n_g(r)$ for gas or $n=n_\ell(r)$ for liquid on the coexistence curve. For the case with $\upsilon_{\rm is}$ we define the grand-potential density,

$$\omega'(r) = g + \upsilon_{\rm is} + \frac{C}{2}|\nabla n|^2 + \frac{\varepsilon}{8\pi}\boldsymbol{E}^2. \tag{2.29}$$

Then we have

$$\Delta_{\rm sol} = 4\pi\int_0^\infty dr r^2[\omega_g'(r) - \omega_\ell'(r)], \tag{2.30}$$

where $n=n_g(r)$ in ω_g' and $n=n_\ell(r)$ in ω_ℓ'. The two terms, $\omega_g'(r)$ and $\omega_\ell'(r)$, in the integrand are mostly canceled in the region $r<\sigma_{\rm is}$. In Fig. 6 we show $\beta\Delta_{\rm sol}$ on the coexistence curve for $A=5$ (left) and 50 (right). As explained in Sec. II B, Eq. (2.17), the Born approximation, much overestimates $\Delta_{\rm sol}$ in a strong solvation.

III. ION-INDUCED NUCLEATION IN GAS

A. Critical droplet and KO approximation

In nucleation theory[21,27,28] crucial is the free-energy increase to create a critical droplet, which will be written as W_c and will be called the nucleation barrier. Its definition for ion-induced nucleation will follow in Eq. (3.3) below. The nucleation rate J is the birth rate of droplets of the new phase with radius larger than the critical radius R_c emerging in a metastable state per unit volume. It is approximately given by

$$J = J_0 \exp(-\beta W_c) \tag{3.1}$$

independently of the details of the dynamics. Here J_0 is a microscopic coefficient (of the order n/τ_m with τ_m being a microscopic time away from the critical point) and $\beta = 1/k_BT$. A unique aspect of nucleation in gaseous polar fluids is that the solvated region around an ion can serve as a seed of a nucleating liquid droplet in a metastable state. This leads to a considerable decrease in W_c and a dramatic increase in J in the presence of a small amount of ions.

Mathematically, the extremum condition (2.21) holds also for the critical-droplet profile,

$$n = n_{\rm cri}(r), \tag{3.2}$$

which assumes liquid values for $r \lesssim R_c$ and tends to a metastable gas density n_∞ at large $r \gg R_c$. This solution of Eq. (2.21) is unstable; that is, if we superimpose a small density perturbation inside a critical droplet, $\Delta\Omega$ (or $\Delta\Omega'$) decreases.[29] In Fig. 7 with $\upsilon_{\rm is}$ being included, the normalized density $\phi(r)=\upsilon_0 n_{\rm cri}(r)$ for a critical droplet is displayed around an ion with $A=50$ for $T/T_c=0.928$ (left) and 0.675 (right). The dotted and broken lines represent the solvation profile in a metastable gas and in a stable liquid, respectively. Here $\delta T/T_c$ is −0.011 (left) and −0.046 (right), so R_c is larger for the former case.

The nucleation barrier W_c is then written as

$$W_c = \begin{cases} (\Delta\Omega)_{n=n_{\rm cri}} - (\Delta\Omega)_{n=n_g} & \text{without } \upsilon_{\rm is}, \\ (\Delta\Omega')_{n=n_{\rm cri}} - (\Delta\Omega')_{n=n_g} & \text{with } \upsilon_{\rm is}, \end{cases} \tag{3.3}$$

where $n_{\rm cri}(r)$ is the critical-droplet solution and $n_g(r)$ is the inhomogeneous solution for the metastable gas. In terms of ω' in Eq. (2.29) we have

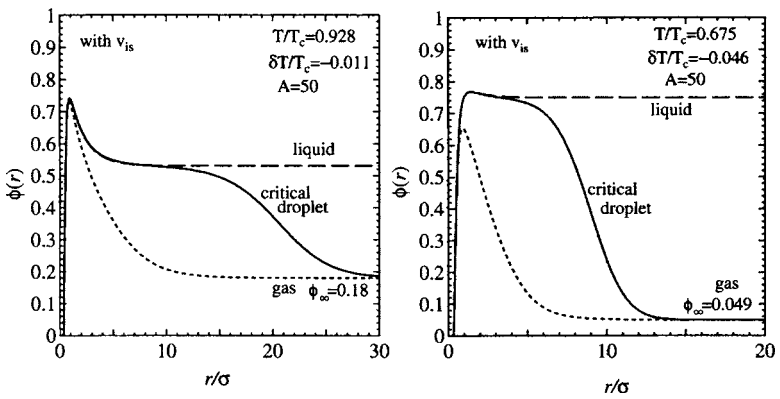

FIG. 7. Normalized density $\phi(r)$ around an ion with $A=50$ in a metastable gas with $\phi_\infty=0.18$ (dotted line) and in the corresponding liquid (broken line) at $T/T_c=0.928$ (left) and 0.675 (right). Also shown is the critical droplet obtained from Eq. (2.19). Here $\upsilon_{\rm is}$ is present and $n(r)$ tends to zero at small r.

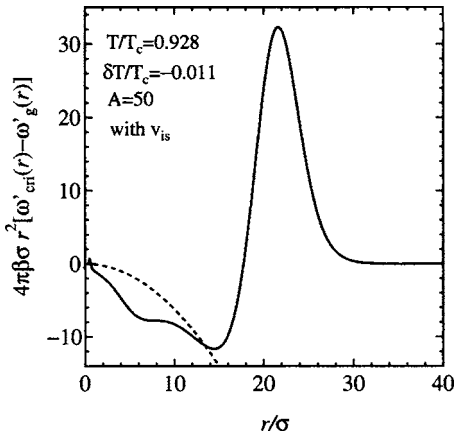

FIG. 8. $4\pi\beta\sigma r^2[\omega'_{\rm cri}(r)-\omega'_g(r)]$, whose integration with respect to r/σ gives βW_c as in Eq. (3.4). The dotted line represents $-4\pi(\beta\sigma\delta\mu)r^2$ where $\delta\mu$ appears in Eq. (3.6). The difference between these curves within the droplet is the solvation contribution.

$$W_c = 4\pi\int_0^\infty dr r^2[\omega'_{\rm cri}(r)-\omega'_g(r)], \tag{3.4}$$

for the case with $v_{\rm is}$. Here $n=n_{\rm cri}(r)$ in $\omega'_{\rm cri}$ and $n=n_g(r)$ in ω'_g. The numerical calculation of W_c in this manner will be referred to as the KO approximation. In Fig. 7 the calculated βW_c is 50.58 (left) and 101.24 (right). In Fig. 8 we show the dimensionless quantity $4\pi\beta\sigma r^2[\omega'_{\rm cri}(r)-\omega'_g(r)]$ for the case of $T/T_c=0.928$ (left) in Fig. 7, which is the integrand in Eq. (3.4) multiplied by $\beta\sigma$. It consists of a negative part within the droplet $r\lesssim R_c$ and a positive surface part at $r\sim R_c$, and its integral with respect to r/σ is equal to $\beta W_c\sim 50$.

B. KO′ approximation

In the KO approximation for W_c we need to calculate $n_{\rm cri}(r)$ for each given set of the parameters δT, A, and R_i. We here propose a simpler (KO′) approximation valid for shallow quenching. That is, we set

$$W_c = -\Delta_{\rm sol} + W_c^0, \tag{3.5}$$

where $\Delta_{\rm sol}$ is the constant independent of R defined by Eq. (2.28) and W_c^0 is the nucleation free energy in the absence of ions or for homogeneous nucleation. The first term arises from the difference between the solvation free energy in gas and liquid, which may be equated to the values on the coexistence curve for shallow quenching as indicated by Fig. 3. In curves in Figs. 9 and 10 to follow, W_c^0 will be numerically obtained from Eq. (2.21) for pure fluids or for $Ze=0$ and $v_{\rm is}=0$.

For large droplets ($R\gg\xi$) we may propose the following droplet free energy:

$$W_{\rm KO}(R) = -\Delta_{\rm sol} + 4\pi\gamma R^2 - \frac{4\pi}{3}\delta\mu R^3. \tag{3.6}$$

The last two terms have the meaning of the minimum work needed to form a droplet with radius R in homogeneous nucleation.[28] Namely, the second term is the surface part with γ being the surface tension. The third term with $\delta\mu=-g(n_\ell)$ is the bulk part, which is negative or $\delta\mu>0$ in metastable states. Notice that the dotted curve in Fig. 8 represents $-4\pi(\beta\sigma\delta\mu)r^2$. See Appendix B for more discussions on $\delta\mu$. This $W_{\rm KO}(R)$ is maximized at the Kelvin radius,

$$R_K = 2\gamma/\delta\mu, \tag{3.7}$$

which is the critical radius in homogeneous nucleation. The maximum value is the nucleation barrier,

$$W_c \cong -\Delta_{\rm sol} + \tfrac{4}{3}\pi\gamma R_K^2. \tag{3.8}$$

In this simple case Eq. (3.1) may be rewritten as

$$\delta\mu = (16\pi\beta\gamma^3/3)^{1/2}/[\ln(J_0/J) + \beta\Delta_{\rm sol}]^{1/2}. \tag{3.9}$$

An appreciable droplet formation is observed for a sufficiently large nucleation rate J dependent on the experimental method ($\sim 1/{\rm cm}^3$ sec, say) and the above formula determines the so-called cloud point of nucleation.[21]

C. Thomson approximation

Since Thomson's work,[2] the droplet free energy for large R has been assumed to be of the form[3,30,31]

$$W_T(R) = -\frac{\alpha}{R_i} + \frac{\alpha}{R} + 4\pi\gamma R^2 - \frac{4\pi}{3}\delta\mu R^3, \tag{3.10}$$

where α is written in terms of the dielectric constant in gas ε_g and in liquid ε_ℓ as

$$\alpha = \tfrac{1}{2}Z^2e^2(1/\varepsilon_g - 1/\varepsilon_\ell). \tag{3.11}$$

The first two terms in Eq. (3.10) represent the difference of the electrostatic free energy F_e between the two phases,

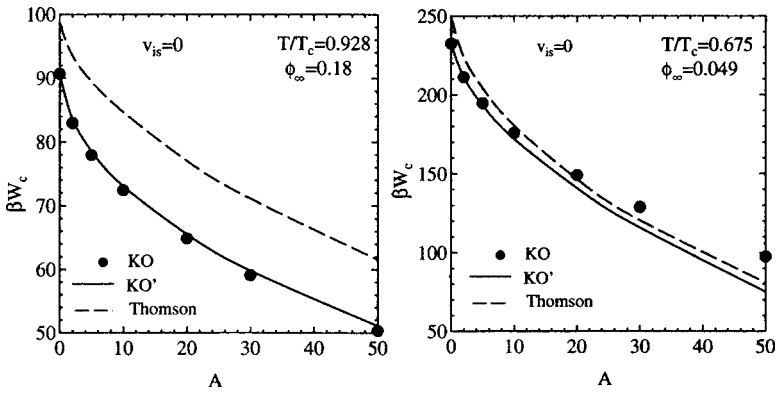

FIG. 9. Normalized free energy βW_c without $v_{\rm is}$ at $T/T_c=0.928$ (left) and 0.675 (right) as a function of A. The dots (●) (KO) are obtained by solving Eq. (2.21). The solid line (KO′) is calculated from Eq. (3.14), while the broken line (Thomson) is from the first line of Eq. (3.16).

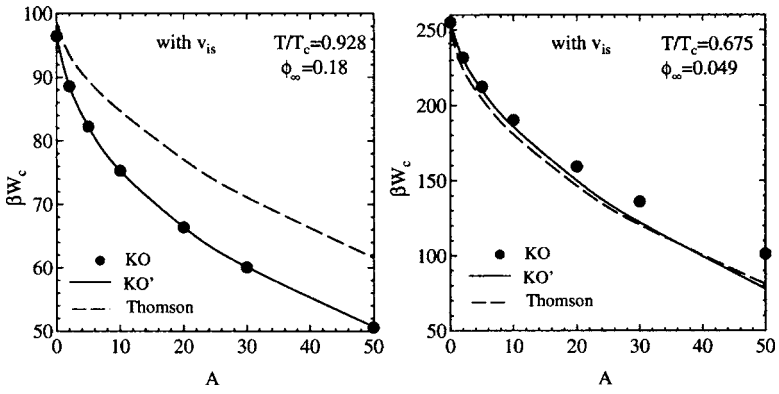

FIG. 10. Normalized free energy βW_c with v_{is} at T/T_c=0.928 (left) and 0.675 (right) as a function of A. The dots (●) (KO) are obtained by solving Eq. (2.21). The solid line (KO′) is calculated from Eq. (3.14), while the broken line (Thomson) is from the first line of Eq. (3.16).

$$(\Delta F_e)_{\mathrm{Born}} = -\int_{R_i}^{R} dr \frac{\alpha}{r^2}, \tag{3.12}$$

where the upper bound of the integration is R since $\varepsilon(n)$ changes from ε_ℓ to ε_g at $r=R$ with increasing r. The first term in Eq. (3.10) arises from the lower bound and turns out to be the Born approximation of $-\Delta_{\mathrm{sol}}$ in Eq. (2.28).

Thomson[2] found that the sum of the second and third terms on the right-hand side of Eq. (3.10) is minimized at the Rayleigh radius,[32]

$$R_R = (\alpha/8\pi\gamma)^{1/3}. \tag{3.13}$$

He concluded that an ion in gas is surrounded by a spherical liquid region with radius R_R. However, as estimated by Thomson himself, R_R is only about 3 Å for an ion with $Z=1$ in room-temperature water vapor, while Eq. (3.10) should be valid only for large R. For not very large Z we can see that R_R cannot exceed even the interface thickness at any temperatures.[33] In addition, the use of the surface tension makes his argument applicable only in the region $\delta T \leqq 0$. As shown in Fig. 3, the solvation density profiles of small ions should be continuous through the coexistence curve. Obviously, the second term ($\propto R^{-1}$) in Eq. (3.10) is negligible for $R \gg R_R$ and the Thomson theory is not well justified (if applied to microscopic ions).

We explain how the nucleation free energy W_c is calculated in the Thomson theory.[3] The extremum condition $\partial W_T(R)/\partial R=0$ becomes $x^3(1-x)=\alpha^*$ with $x=R/R_K$, where

$$\alpha^* = \alpha/8\pi\gamma R_K^3 = (R_R/R_K)^3. \tag{3.14}$$

We can see that $W_T(R)$ has a maximum $W_{\max}$ and a minimum $W_{\min}$ for

$$\alpha^* < 27/256 \quad \text{or} \quad R_R/R_K < 3/4^{4/3}. \tag{3.15}$$

Since R_R is microscopic for small Z, we have $\alpha^* \ll 1$ for shallow quenching. Obviously, the radius giving the maximum is nothing but the critical radius R_c. For small α^*, R_c behaves as $R_c=R_K(1-\alpha^*+\cdots)$, while the radius giving the minimum is nearly equal to R_R. If Thomson's idea is extended, a preexisting *liquid droplet* with radius R_R grows into a larger liquid droplet in nucleation. Within his theory, the nucleation barrier is given by[3]

$$W_c = W_{\max} - W_{\min} = \tfrac{4}{3}\pi\gamma R_K^2(1+8\alpha^*) - 12\pi\gamma R_R^2 + \cdots. \tag{3.16}$$

In the first line the first term in Eq. (3.10) is canceled to vanish. The second line is an expansion in powers of $(\alpha^*)^{1/3}$ for small α^*. This approximation was adopted in Ref. 3, but it is not well justified for small R_R and hence for small ions.

D. Numerical results for W_c

Without v_{is} in Fig. 9 and with v_{is} in Fig. 10, the normalized nucleation barrier βW_c is plotted as a function of A at T/T_c=0.928 (left) and 0.675 (right). The profiles of the critical droplets are shown in Fig. 7 at $A=50$ for these temperatures. The dots (•) (KO) are obtained from the profile of the critical droplet satisfying Eq. (2.21). The solid line represents βW_c in Eq. (3.5) (KO′), while the broken line represents βW_c in Eq. (3.16)(Thomson). It is remarkable that there is no essential difference between Fig. 9 without v_{is} and Fig. 10 with v_{is}. (i) For T/T_c=0.928, good agreement is obtained between the KO result and the KO′ result because of relatively large R_c, while the Thomson result is larger by about ten. For example, for T/T_c=0.928 and $A=50$ in Fig. 10, βW_c is given by 50.58 (KO), 50.71 (KO′), and 61.59 (Thomson). (ii) For T/T_c=0.675, the KO values of βW_c agree with the KO′ values for $A \lesssim 10$, but become considerably larger for $A \gtrsim 20$. In fact, βW_c is given by 101.24 (KO), 77.80 (KO′), and 80.96 (Thomson) for T/T_c=0.675. In this lower-temperature case R_c is of the order R_{shell}, as shown in Fig. 7, and hence the expression of $W_T(R)$ in Eq. (3.10) should not be a good approximation.

For these two temperatures βW_c decreases with increasing A. At small $A(\lesssim 5)$ the curves are rather steep mainly due to the small size of $R_i/\sigma=0.3$ in Eq. (2.24). In the density-functional theory Kusaka *et al.*[6] calculated W_c for $R_i=\sigma$ as a function of another parameter χ ($=Zep_0/\sigma^2 k_B T_c$, with p_0 being the dipole moment of a polar molecule) and found that it is rather weakly dependent on χ for small χ.

IV. SUMMARY AND CONCLUDING REMARKS

In summary, we have presented a simple theory of ion-induced nucleation in polar one-component fluids, where the effect of electrostriction is crucial. We summarize our main results.

(i) We use a simple continuum model, where the electrostatic free energy is given by Eq. (2.5), and the grand-potential increase due to an ion is given by Eq. (2.15) or Eq. (2.18). Particularly, we use the Harris-Alder formula (2.7) for the dielectric constant as a function of the density and the van der Waals form for the Helmholtz free-energy density in Eq. (2.8). The density profiles around an ion are numerically obtained as illustrated in Figs. 3 and 7.

(ii) We have proposed the droplet free energy $W_{\mathrm{KO}}(R)$ in Eq. (3.6) for a large liquid droplet in a metastable gas with an ion at its center. It is remarkable that the difference in solvation in gas and in liquid gives rise to the negative background contribution $-\Delta_{\mathrm{sol}}$, which much favors nucleation around an ion in a metastable gas.

(iii) The nucleation barrier W_c has been calculated in three manners. In our Ginzburg-Landau scheme we have directly sought an unstable solution of Eq. (2.21) to obtain the dots (•) (KO) in Figs. 9 and 10. It may also be calculated more approximately using Eq. (3.5) (KO′) or the first line of Eq. (3.16) (Thomson). They yield the solid lines and the dotted lines in Figs. 9 and 10, respectively. We have found that the KO′ result is close to the directly calculated result (KO) for relatively large critical radius R_c if the background is chosen to be $-\Delta_{\mathrm{sol}}$.

(iv) We have presented the density profiles in Figs. 4 and 7, which tend to zero at the ion center owing to the pair potential v_{is}. However, we have obtained essentially the same results for the free-energy barrier W_c in Fig. 9 without v_{is} and in Fig. 10 with v_{is}.

Finally, we make some remarks.

(i) We have used the Ginzburg-Landau theory with the simple gradient free energy. However, far from the critical point as in the case of $T/T_c=0.675$, the density-functional theory[6,27,34] with a nonlocal pair interaction would give more improved results.

(ii) Because of its simplicity we have used the macroscopic linear dielectric formula (2.7) even very close to the ion. This has been the approach in the previous continuum theories,[2,10] but it is not well justified. In particular, we should examine the effect of nonlinear dielectric saturation in solvation, which gives rise to a decrease in the effective dielectric constant close to the ion.[15,16]

(iii) The difference Δ_{sol} of the solvation free energies in Eq. (2.28) is a relevant parameter generally in ionic solutions in two-phase states, although the present work has treated the case of a single ion. For example, it gives rise to ion-density differences inside and outside a wetting layer.

(iv) Obviously W_c tends to zero on approaching the critical point. However, this is the result for a single ion. We point out that even a small concentration of ions can drastically alter the phase behavior of near-critical polar fluids.[13]

(v) We can also construct a theory of ion-induced nucleation in binary fluid mixtures.[13]

ACKNOWLEDGMENTS

We would like to thank M. Anisimov for valuable discussions and for providing us a copy of the article by Fernandez *et al.*[17] This work was supported by Grants in Aid for Scientific Research and for the 21st Century COE "Center for Diversity and University in Physics" from the Ministry of Education, Culture, Sports, Science and Technology of Japan.

APPENDIX A: SURFACE TENSION

Here we consider the surface tension γ in the absence of ions in our model in the mean-field theory.[21] To have a planar interface we assume that the fluid is on the coexistence curve or the pressure is given by $p=p_{\mathrm{cx}}(T)$ with the temperature below T_c. The grand-potential density

$$g(n)=f(n)-\mu_{\mathrm{cx}}n+p_{\mathrm{cx}} \tag{A1}$$

is minimized at $n=n_g$ and n_ℓ on the coexistence curve, with the minimum value being zero. For our van der Waals free energy f in Eq. (2.8) and the gradient free energy in Eq. (2.15), a planar interface profile $n=n(x)$ changing along the x axis satisfies $\partial g/\partial n=C\partial^2 n/\partial x^2$, yielding $g=C(\partial n/\partial x)^2/2$. Then γ is expressed as

$$\gamma=\int_{-\infty}^{\infty}dx[g+C(\partial n/\partial x)^2/2]=(2C)^{1/2}\int_{n_g}^{n_\ell}dn[g(n)]^{1/2}. \tag{A2}$$

In the vicinity of the critical point it follows the power-law behavior,

$$\gamma=C_s\epsilon_{\mathrm{vw}}(1-T/T_c)^{3/2}/\sigma^2, \tag{A3}$$

where C_s is a constant. Widely in the range $T/T_c\gtrsim 0.6$, however, we have found that γ numerically calculated from the second line of Eq. (A2) with Eq. (2.13) can be fitted to Eq. (A3) within a few percents if we set

$$C_s=3.0. \tag{A4}$$

With this C_s Eq. (A2) yields $\gamma\cong 235(1-T/T_c)^{3/2}$ dyn/cm where we use the values of ϵ_{vw} and σ given in Sec. II B for water.

Experimentally,[23] the surface tension of water behaves as $215(1-T/T_c)^{2\nu}$ dyn/cm with $\nu\cong 0.63$ in the range $1-T/T_c\lesssim 0.1$. However, the calculated γ fairly agrees with the experimental surface tension of water far from the critical point. For example, at $T/T_c=0.675$, our γ is 42.5 dyn/cm, while the experimental value is 44.6 dyn/cm. Since $C_s\propto C^{1/2}$, our choice of C in Eq. (2.21) is justified.

APPENDIX B: BEHAVIOR OF $\delta\mu$

We examine the behavior of $\delta\mu=-g(n_\ell)$ in Eq. (3.6), first fixing T below T_c. From Eq. (2.16) it becomes

$$\delta\mu = p_\ell - p_\infty + n_\ell(\mu_\infty - \mu_\ell)$$
$$= -(f(n_\ell) - \mu_{cx}n_\ell + p_{cx}) + n_\ell(\mu_\infty - \mu_{cx}) - (p_\infty - p_{cx}). \quad \text{(B1)}$$

The quantities with the subscript ℓ, ∞, and cx are those within the liquid droplet, in the metastable gas, and on the coexistence curve, respectively. See Ref. 28 for a derivation of the first line of Eq. (B1) from statistical-mechanical principles. In the second line, the first term is negligible since n_ℓ is close to the liquid density on the coexistence curve. In the limit $p_{cx}-p_\infty \to 0$, the Gibbs-Duhem relation gives

$$\delta\mu \cong (\Delta n/n_g)(p_\infty - p_{cx}), \quad \text{(B2)}$$

where $\Delta n = n_\ell - n_g$. This relation is useful near the critical point. For dilute gas we have $p \cong k_B T n$ and $\mu_\infty - \mu_{cx} = \int_{p_{cx}}^{p_\infty} dp n(p)^{-1} \cong k_B T \ln(p_\infty/p_{cx})$ at fixed T. If $n_g \ll n_\ell$, the second term is much larger than the third on the right-hand side of Eq. (B1), leading to the well-known expression[3,4]

$$\delta\mu \cong k_B T n_\ell \ln(p_\infty/p_{cx}). \quad \text{(B3)}$$

In real experiments the temperature T_∞ in gas (written as T in the above discussion) may also be changed. Let us consider a reference state at temperature T_0 and pressure $p_0 = p_{cx}(T_0)$ on the coexistence curve. In such cases we should replace $p_\infty - p_{cx}(T_0)$ in the above formulas by $p_\infty - p_{cx}(T_0) - (\partial p/\partial T)_{cx}(T_\infty - T_0) \cong p_\infty - p_{cx}(T_\infty)$ for shallow quenching, where $(\partial p/\partial T)_{cx}$ is the derivative along the coexistence curve.[21] In Fig. 2, for example, the temperature is changed across the coexistence curve at a fixed average density n_0 or at a fixed system volume, where we may set $T_0 = T_{cx}(n_0)$. This means $p_\infty - p_{cx}(T_0) = (\partial p/\partial T)_n (T_\infty - T_0)$ in the gas, leading to $\delta\mu = [\Delta n(\partial n/\partial T)_{cx}/n_g^2 K_T](T_0 - T_\infty)$ in terms of the compressibility K_T in the gas. Here use is made of the thermodynamic relation $(\partial p/\partial T)_n - (\partial p/\partial T)_{cx} = -(\partial n/\partial T)_{cx}/nK_T$ on the coexistence curve [see Eq. (2.2.39) of Ref. 21].

[1] C. T. R. Wilson, Philos. Trans. R. Soc. London, Ser. A **189**, 265 (1897).
[2] J. J. Thomson, *Conduction of Electricity through Gases* (Cambridge University Press, Cambridge, 1906), Sec. 92.
[3] T. Seto, K. Okuyama, L. de Juan, and J. Fernández de la Mora, J. Chem. Phys. **107**, 1576 (1997).
[4] G. Gamero-Gastano and J. Fernandez de la Mora, J. Chem. Phys. **117**, 3345 (2002).
[5] J. N. Israelachvili, *Intermolecular and Surface Forces* (Academic, London, 1991).
[6] I. Kusaka, Z.-G. Wang, and J. H. Seinfeld, J. Chem. Phys. **102**, 913 (1995).
[7] I. Kusaka, Z.-G. Wang, and J. H. Seinfeld, J. Chem. Phys. **103**, 8993 (1995).
[8] K. J. Oh, G. T. Gao, and X. C. Zeng, Phys. Rev. Lett. **86**, 5080 (2001).
[9] E. Broadskaya, A. P. Lyubartsev, and A. Laaksonen, J. Chem. Phys. **116**, 7879 (2002).
[10] M. Born, Z. Phys. **1**, 45 (1920).
[11] The free energy due to the polarization and the charge[12] is $F_e = \int d\boldsymbol{r}(\boldsymbol{P}^2/2\chi + \boldsymbol{E}^2/8\pi)$ with $\nabla\cdot(\boldsymbol{E}+4\pi\boldsymbol{P}) = 4\pi\rho$. For $\boldsymbol{P} = \chi\boldsymbol{E}$ we obtain Eqs. (2.1) and (2.5). If $\boldsymbol{P}=0$, it is equal to the vacuum result $Z^2e^2/2R_B$ for a single ion. If $\boldsymbol{P} = \chi\boldsymbol{E}$ without electrostriction, it is equal to $\Delta\Omega_{Born}$ in Eq. (2.17). In literature (Refs. 5 and 10) the difference of these two quantities is the Born formula for the solvation free energy.
[12] A. Onuki, in *Nonlinear Dielectric Phenomena in Complex Liquids*, NATO Science Series II: Mathematics, Physics and Chemistry, edited by S. J. Rzoska and S. J. Zhelezny (Kluwer Academic, Dordrecht, 2004), Vol. 157.
[13] A. Onuki and H. Kitamura, J. Chem. Phys. **121**, 3143 (2004).
[14] Y. Marcus, Chem. Rev. (Washington, D.C.) **88**, 1475 (1988).
[15] M. H. Abraham, J. Liszi, and L. Meszaros, J. Chem. Phys. **70**, 2491 (1979).
[16] L. Sandberg and O. Edholm, J. Chem. Phys. **116**, 2936 (2002).
[17] D. P. Fernandez, A. R. H. Goodwin, E. W. Lemmon, J. M. H. Levelt Sengers, and R. C. Williams, J. Phys. Chem. Ref. Data **26**, 1125 (1997).
[18] F. E. Harris and B. J. Alder, J. Chem. Phys. **21**, 1031 (1953).
[19] J. G. Kirkwood, J. Chem. Phys. **7**, 911 (1939).
[20] D. G. Archer and P. Wang, J. Phys. Chem. Ref. Data **19**, 371 (1990).
[21] A. Onuki, *Phase Transition Dynamics* (Cambridge University Press, Cambridge, 2002).
[22] A. K. Wyczalkowska, Kh. S. Abdulkadirova, M. A. Anisimov, and J. V. Sengers, J. Chem. Phys. **113**, 4985 (2000).
[23] S. B. Kiselev and J. F. Ely, J. Chem. Phys. **119**, 8645 (2003). These authors wrote the gradient free-energy density as $c_0|\nabla n|^2/n_c^2$ and found that $c_0 \sim k_B T n_c^{1/3}$ gives good estimates of the surface tension over a wide temperature range for water. This gives $C/k_B T\sigma^5 \sim 2\times 3^{5/3} \cong 12.5$ from $C = 2c_0/n_c^2$ and Eq. (2.13).
[24] In discussing the droplet growth we need to consider the inhomogeneity of the temperature induced by latent heat absorption or generation at the interface (Ref. 21).
[25] In Eq. (2.17) we obtain $R_B = (5/6)R_i$ from Eq. (2.5) if the integration is performed also in the region $r < R_i$ (Ref. 13).
[26] If the radius R_i of the charged particle is much larger than the microscopic radius σ of the fluid, a first-order prewetting transition should take place in the off-critical condition near the coexistence curve. A similar layer transition was predicted for liquid crystals: J.-I. Fukuda, H. Stark, and H. Yokoyama, Phys. Rev. E **69**, 021714 (2004).
[27] D. W. Oxtoby, J. Phys.: Condens. Matter **4**, 7627 (1992).
[28] P. G. Debenedetti, *Metastable Liquids* (Princeton University, Princeton, NJ, 1996).
[29] In dynamics growing or shrinking of the droplet occurs depending on whether the added particle number is positive or negative. For example, this can be verified if we assume the time-evolution equation $\partial n/\partial t = \nabla^2 \delta(\Delta\Omega')/\delta n$.
[30] A. B. Nadykto and F. Yu, Phys. Rev. Lett. **93**, 016101 (2004).
[31] S. M. Kathmann, G. K. Schenter, and B. C. Garrett, Phys. Rev. Lett. **94**, 116104 (2005).
[32] Lord Rayleigh, *The Theory of Sounds* (Dover, New York, 1945), Sec. 364. Rayleigh examined surface deformations of a charged liquid droplet in gas and found that it breaks into smaller droplets when its radius is larger than R_R in Eq. (3.13).
[33] Near the critical point we obtain $R_R/\xi \sim (1-T/T_c)^{(\nu+\beta)/3}$, where $\xi \propto (1-T/T_c)^{-\nu}$ is the correlation length with $\nu \cong 0.63$ and $\beta \cong 0.33$ being the critical exponents (Ref. 21). The interface thickness is of the order ξ.
[34] D. W. Oxtoby and R. Evans, J. Chem. Phys. **89**, 7521 (1988).